Eur. Phys. J. B **37**, 109–115 (2004)
DOI: 10.1140/epjb/e2004-00035-y

THE EUROPEAN PHYSICAL JOURNAL B

Characterizing neuromorphologic alterations with additive shape functionals

M.S. Barbosa[1,a], L. da F. Costa[1], E.S. Bernardes[2], G. Ramakers[3], and J. van Pelt[3]

[1] Cybernetic Vision Research Group, GII-IFSC, Universidade de São Paulo, São Carlos, SP, Caixa Postal 369, 13560-970, Brasil
[2] DFCM-IFSC, Universidade de São Paulo, São Carlos, SP, Caixa Postal 369, 13560-970, Brasil
[3] Neurons and Network, Netherlands Institute of Brain Research, Meibergdreef 33, 1105 AZ Amsterdam, The Netherlands

Received 31 July 2003 / Received in final form 10 November 2003
Published online 19 February 2004 –

Abstract. The complexity of a neuronal cell shape is known to be related to its function. Specifically, among other indicators, a decreased complexity in the dendritic trees of cortical pyramidal neurons has been associated with mental retardation. In this paper we develop a procedure to address the characterization of morphological changes induced in cultured neurons by over-expressing a gene involved in mental retardation. Measures associated with the multiscale connectivity, an additive image functional, are found to give a reasonable separation criterion between two categories of cells. One category consists of a control group and two transfected groups of neurons, and the other, a class of cat ganglionary cells. The reported framework also identified a trend towards lower complexity in one of the transfected groups. Such results establish the suggested measures as an effective descriptors of cell shape.

PACS. 87.80.Pa Morphometry and stereology – 87.19.La Neuroscience

1 Introduction

Classical investigations in neuroscience have added a large amount of descriptive data to the knowledge of the mammalian neural system and ultimately of the functioning of the brain. In recent years the use of computer and algorithmical methods has been incorporated into the biological sciences with the aim of achieving quantitative analysis and modelling. Being no exception to this important tendency, mathematic-computational investigations in neuroscience are still in an incipient stage, with many challenging questions and potential for important results. While the effort to model quantitatively the emergent features of a neural system or element (e.g. a single cell) involves its own technical difficulties, neuroinformatics has already led to important results regarding the interplay between the morphology of dendrites and their firing patterns [1]. One difficult aspect implied by the use of computers in neuroanatomy is the relatively limited availability of accurate spatial data of real dendritic arborizations for diverse morphological classes. The alternative approach of generating morphologically realistic neurons has been successfully carried out by using a complementary approach based either on recursive [2] or topological [3,4] algorithmic implementation.

The anatomic details of the neuronal cells have been shown to represent a relevant feature, for phylogenic and ontogenic studies, in the diagnosis of diseases and in investigating the interplay between form and function [4–6]. With the availability on the Internet of combined databases of virtual and real (histochemically marked) neurons, the analysis or morphological characterization of newly acquired neuronal information can now be the subject of systematic processing by computer methods, provided suitable shape descriptors are identified and applied.

There is a current interest in many branches of Physical and, more recently, Biological sciences to study in a quantitative way the geometrical outline of structures, both static and in development, and from that knowledge to probe further into the functioning and justification of those forms. Examples of results of such a quest in biology ranges from the elucidation of the Fibonacci spirals emerging in sunflowers [7,8] to the fractal characterization of the nature of many botanical plants [9]. For over a century the search aimed at establishing a relationship between the form and function of neuronal cells has challenged and stimulated researchers, starting from the pioneering efforts of Ramón y Cajal [10]. While many diseases have been diagnosed based on the visual perception of morphological alterations in general tissue morphology, automated approaches remain promising subjects of research, with many potentially important applications.

Although it is now generally accepted that dendritic morphology plays a crucial role in the functioning of the neural cell and ultimately in the behaviour of the neural

[a] e-mail: marconi@if.sc.usp.br

system [1,11–14], there is no deterministic way to choose the best quantitative descriptor of the geometry or topology of single neurons. In order to be particularly useful, such descriptors should correlate in some way with the respective performed functions and behaviour, allowing abnormalities and specific divergences from a healthy state or development to be clearly identified. An additional benefit of such an investigation of the physical basis of neuronal shape and growth is the possibility for investigating, through modelling, the relationship between neuronal shape and function.

The study of biological forms requires the selection of shape descriptors or shape functionals that fulfil a set of requests. First, measures are expected to be objective and fast (in order to treat a representative number of cases), while retaining comprehensiveness and being potentially discriminative. In addition, such measures should lead to meaningful biological interpretations. An important theoretical issue is the relative degeneracy of a set of measures, a concept that reflects the fact that many different forms or shapes produces the same or approximated measures. It has been experimentally shown [5,15,16] that multiscale analysis tends to augment the resolution power of geometric descriptors and, despite the increased computational demands, this procedure provides useful additional information and characterization of the considered objects. The neuronal cells have, in general, a complex spatial tree-like structure with many dendritic bifurcations leading to efficient spacial coverage, amplifying the influence area and optimally connecting the neuron with a neighbouring cell's dendrites or axons. This structure has been shown to exhibit different levels of partial fractality at different spatial scales [6,17,18].

A recently reported [19,20] procedure for calculating additive shape functionals, known as Minkowski functionals gathered in a framework called Integral-Geometry Morphological Image Analysis, MIA, has been successfully applied to many areas of research including Statistical Physics, Cosmology and Material Sciences [19–23]. A first attempt to bring those morphological concepts into biological sciences, targeting the efficient discrimination of two main types of the domestic cat's ganglionary neuronal cells, has been reported recently [24]. The use of additive functionals is implemented in a pixelwise approach leading to the possibility of straightforwardly obtaining the above mentioned multiscale fractal dimension for complementary shape description. Every additive continuous and motion invariant functionals in the 2D Euclidean plane can be expressed as a combination of three Minkowski functionals which are proportional to a known geometric quantity, namely the metric area and perimeter and the topological Euler connectivity number. This completeness extends to higher dimensions and the geometrical functionals multiplicity is always one plus the dimension of the lattice generalized voxels (e.g. 3 in 2D plane, 4 in 3D space, etc.). While the theory of Integral geometry provides a sophisticated set of results and formulae, the practical implementation of the procedures in Image analysis is relatively simple and efficient [19,20]. The basic ideas of this methodology is described in Section 2 and a simple example is worked out to outline the procedure.

In this paper we investigate the importance of the spatial distribution of branching points in neuronal arborizations to provide a discriminative and informative characterization of the neuronal morphology, with special attention given to additive shape functionals. This novel procedure involves mapping the neuronal image onto a set of points representing its bifurcation pattern, which are subsequently dilated in order to produce a multiscale representation [25], as the Minkowski functionals of such a set of points is recorded. The obtained results substantiate the potential of the above procedure regarding its application to a database of 3 categories of rat neuronal cells and one class of cat ganglion cells. The results are in accordance with the biological importance of the spatial distribution of branches [1,11,12,17,26,27] and provide a discriminative measure for the morphological characterization of the neurons, indicating subtle morphological differences as a consequence of the considered gene transfectation in the rat categories. This suggests that those treatments may not significantly alter the topological aspect of the branching cell form as far as the considered measurements are concerned.

2 Additive functionals

Integral geometry algorithms have been successfully used to characterize morphologically complex patterns where the precise process of formation is not completely known and is a subject of modelling, see for example [28]. The central procedure is the calculation of intrinsic volumes or Minkowski functionals (or yet *querrmassintegrals*), which are a generalization of the usual determination of volume. They can be defined as related to both differential and integral geometry setups.

For the sake of a better explanation, we start with a description of the practical aspect of the adopted procedure. The Minkowski functionals of a body K in the plane are proportional to its area $A(K)$, perimeter $U(K)$ and the connectivity or Euler number $\chi(K)$. The usual definition of the connectivity from algebraic topology in two dimensions is the difference between the number of connected n_c components and the number of holes n_h,

$$\chi(K) = n_c - n_h. \tag{1}$$

So, if K happens to be an image of the number 8 as in Figure 1, its connectivity number would be $\chi(K) = 1 - 2 = -1$. One instance where these functionals appear naturally is while attempting to describe the change in area as the domain K, now assumed to be convex, undergoes a dilation through a parallel set process using a ball B_r of radius r

$$A(K \oplus B_r) = A(K) + U(K)r + \pi r^2. \tag{2}$$

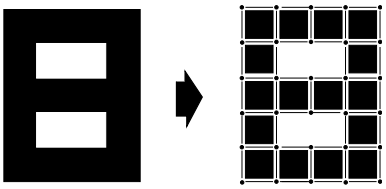

Fig. 1. The disjoint decomposition of a pattern K (left) into a sum $\mathcal{P}$ (right) of disjoint interior elements.

Generalizing to higher dimensions, the change in hyper volume is given by the Steiner formula [21]

$$v^d(K \oplus B_r) = \sum_{\nu=0}^{d} \binom{d}{\nu} W_\nu^{(d)}(K) r^\nu, \tag{3}$$

where the coefficients $W_\nu^{(d)}$ are referred to as Minkowski functionals. For instance in the plane ($d = 2$),

$$W_0^{(2)}(K) = A(K), W_1^{(2)}(K) = \frac{U(K)}{2}, W_2^{(2)}(K) = \chi(K)\pi. \tag{4}$$

Despite the wealth of results and continuum formulae for obtaining these functionals, it is useful to recur to the discrete nature of the binary images we wish to analyse by looking at the distribution of pixels in the planar lattice. On that level, by exploring the additivity of the Minkowski functionals, their determination reduces to counting the multiplicity of basic building blocks that compose the object in a disjointed fashion. Figure 1 illustrates this process. A pixel can be decomposed as a disjointed set of 4 vertices, 4 edges and one square. The same process can be applied to any object in a lattice. The fundamental information needed here is a relationship for the functionals of an open interior of a n-dimensional body K which is embedded into a d-dimensional space

$$W_\nu^{(d)}\left(\breve{K}\right) = (-1)^{d+n+\nu} W_\nu^{(d)}(K), \nu = 0, \ldots, d. \tag{5}$$

As there is no overlap between these building blocks and by the property of additivity of these functionals, for a body P composed of disjointed convex interior pieces $\breve{N}_m$, we may write

$$W_\nu^{(d)}(\mathcal{P}) = \sum_m W_\nu^{(d)}\left(\breve{N}_m\right) n_m(\mathcal{P}),\ \nu = 0, \ldots, d. \tag{6}$$

Where $n_m(\mathcal{P})$ stands for the number of building elements of each type m occurring in the pattern $\mathcal{P}$. For a two-dimensional space, which is our interest regarding the considered neuronal images, we display in Table 1 the value of Minkowski functionals for the building elements in a square lattice of pixels and their direct relation to familiar geometric quantities on the plane. Using the information (with $a = 1$) presented in Table 1 and equation (6) we have

$$A(\mathcal{P}) = n_2,\ U(\mathcal{P}) = -4n_2 + 2n_1,\ \chi(\mathcal{P}) = n_2 - n_1 + n_0. \tag{7}$$

Table 1. Minkowski functionals of open bodies $\breve{N}_m$ which compose a pixel K: $\breve{P}$ (*vertex*), $\breve{L}$ (*open edge*) and $\breve{Q}$ (*open square*).

m	$\breve{N}_m$	$W_0^{(2)} = A(\breve{N}_m)$	$W_1^{(2)} = \frac{1}{2}U(\breve{N}_m)$	$W_2^{(2)} = \pi\chi(\breve{N}_m)$
0	$\breve{P}$	0	0	π
1	$\breve{L}$	0	a	$-\pi$
2	$\breve{Q}$	a^2	$-2a$	π

Going back to Figure 1, we find, for this specific example, as $n_2 = 16, n_1 = 47$ and $n_0 = 30$, that $A = 16, U = 30$ and $\mathcal{X} = -1$. So the procedure to calculate Minkowski functionals of a pattern K has been reduced to the proper counting of the number of elementary bodies of each type that compose a pixel (squares, edges and vertices) involved in the make up of $\mathcal{P}$.

3 Branching point patterns

The existence of profuse branching structures in natural shapes provides evidence of the effectiveness of such shapes in providing an interface with its environment as well as for enabling connections. As pointed out in [12] many conditions may interfere with the morphology of the neuronal tree structure, for instance learning, 'enriched' environment, hormonal fluctuations and levels of bioelectric activity.

The relationship between dendritic morphology and cell functioning, alone or connected in networks, has drawn the attention of scientists leading to a search for a set of measures that would as completely as possible describe the neuronal shape [29]. For example, the dependence of the dendritic diameter on the distance from soma, the relationship between the dendritic diameter before a bifurcation point and the diameter of the two daughters stemming from this point, or the ratio of diameters of daughter dendrites. These are standard examples of a global feature (the first) and two local properties (the following two) one can specify/calculate in describing/analysing a neuronal shape, real or virtual, see [2]. There is a vast recent literature describing shape analysis in general and applied specifically to neuronal shape, see for example [12,27,30] for a general dendritic description, and [18] for multiscale fractality, [15] for wavelets and [5] for bending energy applied to neuromorphometry.

Since the pioneering work of Sholl [26], some authors have mentioned specific situations where the well-known Sholl analysis could lead to degenerate results, assigning to visually different neurons the same (in statistical terms) descriptor values, see [30] for example. The method makes use of a reference point at the soma and draws concentric circles through the dendritic field, while counting the number of intersections within each circle. While this process is easy to implement manually, which may account for its popularity, it clearly fails for asymmetric forms. While alternative approaches [31] report success in improving this setup, we take a different route, abandoning the soma as a reference point.

We start our analysis by taking all bifurcation points and constructing another image keeping the metric relation between these points. Although there are automatic ways of extracting salient points [32–34], we implemented this task in a semi-automated way, which is followed by a sequence of exact dilations (permitted parallel set dilation [25]) of the selected points. Although primarily interested in the connectivity, all Minkowski functionals are calculated by a routine that counts efficiently the multiplicity of the building elements for each neuron image at every radius of dilation as described in Section 2, equation (7). The idea is to use the connectivity of the set of points to capture, at each scale, the spatial relationship of the neuron branching structure. As this measure is invariant to rotation and translation, as well as to scaling, eventual variations of size due to the relative stage of development can be disregarded.

We investigate the morphology of two different categories of cells. One involves cat ganglion alpha cells, which constitutes a class by itself but rather diversified in form, see [24,35]. The other includes foetal rat cerebral cortex neurons cultured in a 2D tissue system [36]. This category is subdivided into three differently treated classes consisting of a control group, a group of neurons transfected with a gene OPHN1 which encodes for oligo-phrenin, and a positive control group transfected with p190 RhoGAP.

Figure 2 shows examples of two treated rat neuronal cells, illustrating the branching selection process adopted in this work. Note that the neuron images have been rescaled in this picture, but the final dilation radius in all processed samples are the same and equal to 30 pixels.

It is important to comment on the complementary nature of the framework proposed in this article with respect to more traditional approaches reported in the literature. When compared to the previous Sholl methodologies, the measurements in our approach adopt multiscale concepts so as to retain as much as possible the metric and global structure, while avoiding the somewhat arbitrary use of the soma as a general reference. In order to express in a more objective and effective way the morphological features of special interest, namely the overall complexity of the neuronal pattern, our procedure was designed from the start to concentrate on the bifurcation points, which are used as primary data. No attempt is made here to achieve completeness in the shape description, or to use the considered measures as features to be incorporated in an algorithm to grow artificial neurons. However, the reported measurements can be useful for statistical validation of such artificial data, in the sense that both the simulated and original neuronal structures should lead to the same probability densities.

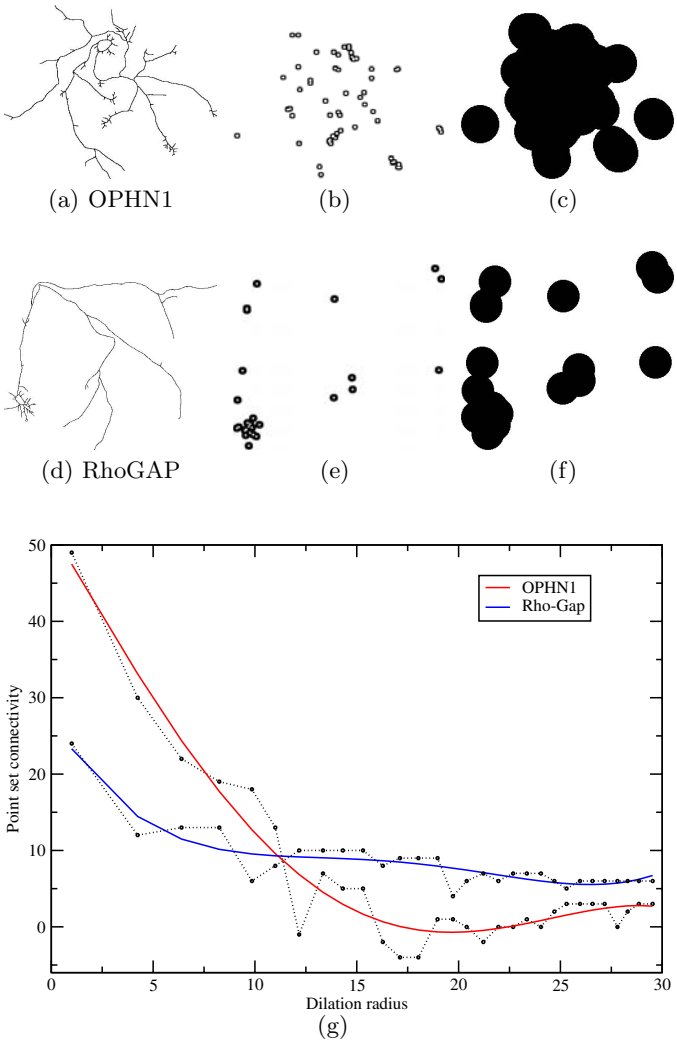

Fig. 2. Isolating morphological information relating to the neuronal branching structure while preserving the metric relationship among the branching points. Each bifurcating point undergoes an exact dilation while its connectivity is recorded as function of the scale parameter. Prototypical transfected rat neuronal cell, a) and d). Extracted pattern of bifurcation points, b) and e). The end of the bifurcation point parallel set dilation procedure, c) and f). The resulting discriminating functional for both neuron types, g).

4 Results

For each cell we calculate multiscale curves of connectivity as shown in Figure 2. As discriminating measurements we take the area under the interpolating curve (its integral) and the standard deviation of the difference between that curve and the original data points. The former can provide information about the overall structure, while the latter characterized the finer details. Having performed similar analysis for area and perimeter functionals, as well as for the multiscale fractality as derived from the area data, we decided to focus on the multiscale connectivity of the branching points set as a descriptor for its relationship to the spatial distribution of branching points and its above average discriminating power.

Our primary concern here is to investigate the effectiveness of the procedure adopted to quantify the subtle morphological aspects that may characterize different cell types while also expressing a biologically relevant attribution of the cell form, namely the distribution of bifurcation points. In this regard, our results, shown by Figure 3, led

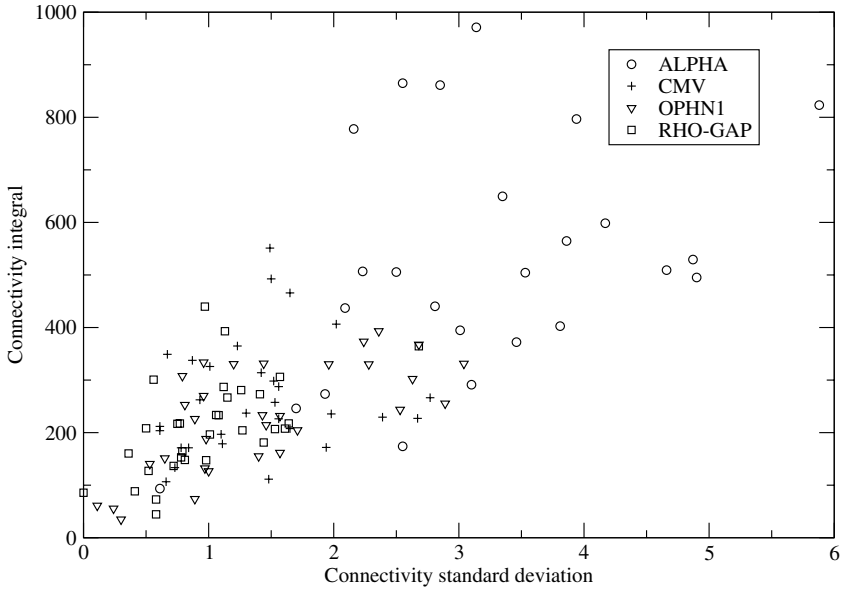

Fig. 3. A discriminative feature space. Most of the Rho-Gap transfected neurons went to the lower left corner of the plot, while the Alpha cat cells are spread by themselves towards higher values. There is a fuzzy display of both control and OPNH-1 samples.

Table 2. Canonical coefficients.

	dim1	dim2
Connectivity Integral	−0.893114489	1.08447785
Connectivity Standard Deviation	−0.003344825	−0.00731277

Table 3. Mahalanobis distance.

	Alpha	CMV	OPHN1	Rho-GAP
Alpha	0.00	6.08	6.53	8.97
CMV		0.00	0.10	0.27
OPHN1			0.00	0.31
Rho-GAP				0.00

to a well-defined separation of the alpha cells in a feature space defined by the integral of the multi scale connectivity and its standard deviation.

Although the three differently treated rat cells are not clearly distinguishable, one group of them, namely the one containing neurons which show over expression of RHO-GAP following transfectation, clearly tends to populate the lower left corner of the feature space. Yet, while high dispersion is shown by the rats sample cells, including the control group which is as much diversified in form as the treated groups, the statistical tendency towards complexity agrees with a previous analysis which focused on the multiscale fractal dimension of this group of cells [37].

Figure 4 shows a scatter plot defined by two canonical discriminant functions (their canonical coefficients are displayed in Tab. 2) for the above selected shape descriptors. The separability in groups is optimized (see Tab. 3 for a quantitative index, the Mahalanobis distance) in such an analysis, leading to a somewhat improved visibility of the above mentioned distinction of the Rho-GAP over expressing set of cells from the others. Nonetheless the other differently treated group mixes up strongly with the control group, as can be verified from Table 4 which presents the plug-in (also called confusion matrix) classification results. As can be seen from this statistical analysis the alpha cat cell is not trivially distinguishable from the others, as shown by the overlaps in both the feature and canonical discriminant scatter plots. While the effectiveness of use of Minkowski functionals (considering the whole cell) has been previously reported [24], the framework developed here is meant to emphasize the distribution of the bifurcation points, in a way similar to that in Sholl's analysis, on the cell morphology.

5 Conclusions

This work describes how promising results have been obtained regarding a novel procedure and measurements for classifying different types of neurons and to reveal morphologically relevant attributes of different classes. Although the subtle morphological variations induced by the treatment of our samples are masked by the statistical distributions and show only a small tendency towards a reduction in complexity, the procedure shows clearly its discriminating power when applied to a well characterized class of alpha cat ganglionary cells. As the considered measurements were designed to express a particular biological aspect of the neuronal geometry, namely the spatial relationship among the branching points, we would expect that this specific trait is not significantly affected by the gene transfectation process. The procedure reported in this paper can be generalised to process 3D Neurons, real or virtual, and can be implemented straightforwardly.

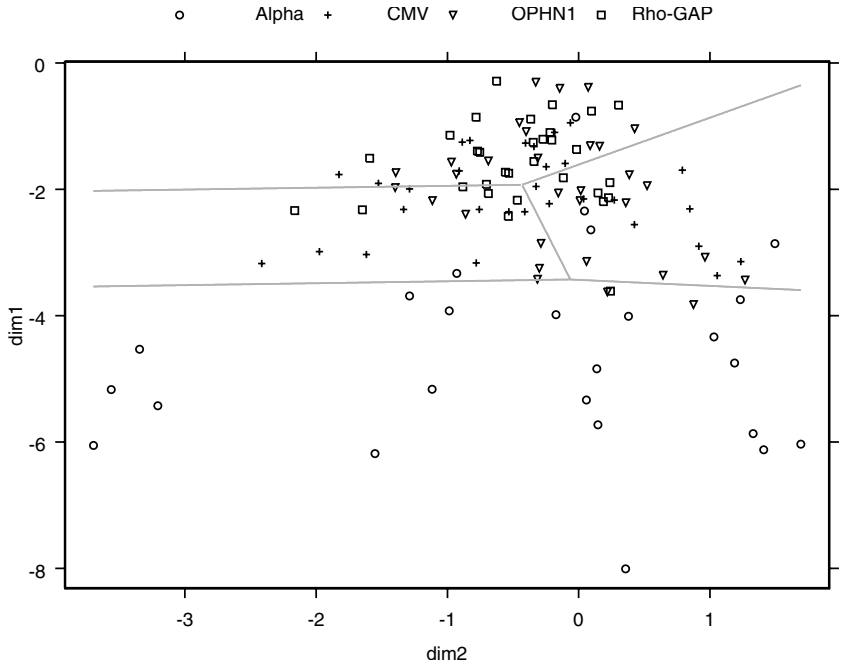

Fig. 4. The discriminative power of the above feature space in depth. A discriminant analysis reveals a reasonable separation among ALPHA and Rho-GAP groups and is not conclusive for the others.

Table 4. Plug-in classification table.

	Alpha	CMV	OPHN1	Rho-GAP	Error	Posterior Error
Alpha	20	1	3	1	0.20	0.25
CMV	0	9	10	11	0.70	0.73
OPHN1	2	6	10	13	0.67	0.65
Rho-GAP	1	6	5	19	0.38	0.41

By extending the present analysis to 3D we suspect that subtle information relating to neuron complexity could be significantly improved.

The authors thank Regina Célia Coelho for kindly providing of the Cat Neurons image database. This work was financially supported by FAPESP (processes 02/02504-01, 99/12765-2 and 96/05497-3) and to CNPQ (process 301422/92-3).

References

1. A. van Ooyen, J. Duijnhouwer, M.W.H. Remme, J. van Pelt, Network Comput. Neural Syst. **13**, 311 (2002)
2. G.A. Ascoli, Anatomical Record (New Anat.) **257**, 195 (1999)
3. J. van Pelt, H.B.M. Uylings, Natural variability in the geometry of dendritic branching patterns, *Modeling in the neurosciences-from ionic channels to neural networks*, edited by R.R. Poznanski (Harwood Academic publishers, Amsterdam, 1999), pp. 79–108
4. L. da F. Costa, R.M. Cesar, R.C. Coelho, J.S. Tanaka, Analysis and synthesis of morphologically realistic neural networks, *Modeling in the neurosciences-from ionic channels to neural networks*, edited by R.R. Poznanski (Harwood Academic publishers, Amsterdam, 1999), pp. 505–527
5. R.M. Cesar, L. da F. Costa, Rev. Sci. Instrum **68**, 2177 (1997)
6. L. da F. Costa, T.J. Velte, J. Comparative Neurology **404**, 33 (1999)
7. S. Douady, Y. Coulder, Phys. Rev. Lett. **68**, 2098 (1992)
8. S. Douady, Y. Coulder, La Recherche **24**, 26 (1993)
9. P. Pruzinkiewicz, A. Lindenmayer, *The algorithmic beauty of the plants* (Springer Verlag, New York, 1990)
10. S.R. y Cajal, *Textura del sistema nervioso del hombre y los vertebrados* (Oxford University Press), pp. 1894–1904 [English translation by N. and L.W. Swanson]
11. S.D. Washington, G.A. Ascoli, J.L. Krichmar, Neurocomputing **32-33**, 261 (2000)
12. H.B.M. Uylings, J. van Pelt, Network: Comput. Neural Syst. **13**, 397 (2002)
13. J.M. Devaud, B. Quenet, J. Gascuel, C. Masson, Bull. Mathematical Biology **62**, 657 (2000)
14. *Neural shape and function*, Special Issue, Brain and Mind **4** (2003)
15. R.M. Cesar, L. da F. Costa, Biological Cybernetics **79**, 347 (1998)
16. A.X. Falcao, L. da F. Costa, B.S. Cunha, Pattern recognition **7**, 1571 (2002)
17. K. Morigiwa, M. Tauchi, Y. Fukuda, Neurosci. Res. **10**, S131–9 (1989)

18. R.C. Coelho, L. da F. Costa, Appl. Signal Processing **3**, 163 (1996)
19. K. Michielsen, H. de Raedt, Phys. Rep. **347**, 461 (2001)
20. K. Michielsen, H. de Raedt, Comput. Phys. Commun. **132**, 94 (2000)
21. L.A. Santaló, *Integral Geometry and Geometric Probability* (Addison-Wesley, Reading, Ma, 1976)
22. D. Stoyan, W.S. Kendall, J. Mecke, *Stochastic Geometry and its applications* (Wiley, West Sussex, England, 1995)
23. K.R. Mecke, Int. J. Mod. Phys. **12**, 861 (1998)
24. M.S. Barbosa, L. da F. Costa, Phys. Rev. E **67**, 061910 (2003)
25. L. da F. Costa, E.T.M. Manoel, Optical Engineering **40**, 1752 (2001)
26. D.A. Sholl, J. Anat. **87**, 387 (1953)
27. H.G. Krapp, B. Hengstenberg, R. Hengstenberg, J. Neurophysiol. **79**, 1902 (1998)
28. K.R. Mecke, Phys. Rev. E **53**, 4794 (1996)
29. D.E. Hillman, *Neuronal shape parameters and substructures as a basis of neuronal form*, *The neurosciences, fourth study program*, edited by F. Schmidt (MIT Press, Cambridge, MA, 1979), pp. 477–498
30. A. Kossel, S. Lowel, J. Bolz, J. Neurosci. **15**, 3913 (1995)
31. H.B.M. Uylings, J. van Pelt, R.W.H. Verwer, P. McConnell, *Statistical analysis of neuronal populations*, *Computer tecniques in neuroanatomy*, edited by J.J. Capowski (Plenum, New York, 1989), pp. 241–64
32. L. da F. Costa, Real-Time Imaging **6**, 415 (2000)
33. L. da F. Costa, Rev. Sci. Instrum.-Computer Vision **66**, 3770 (1995)
34. J.P. Antoine, D. Barache, R.M. Cesar, L. da F. Costa, Signal Processing **62**, 265 (1997)
35. R.C. Coelho, V.D. Gesu, G.L. Bosco, J.S. Tanaka, C. Valenti, Real-Time Imaging **8**, 213 (2002)
36. G.J.A. Ramakers, J. Winter, T.M. Hoogland, M.N. Lequin, P. van Hulten, Dev. Brain Res. **108**, 205 (1998)
37. L da F. Costa, E.T.M. Manoel, F. Faucereau, J. Chelly, J. van Pelt, G. Ramakers, Network: Comput. Neural Syst. **13**, 283 (2002)